Synthesis of Metal/Bimetal Nanowires and Their Applications as Flexible Transparent Electrodes

Xiao Wang, Ranran Wang, Liangjing Shi, and Jing Sun**

As a potential alternative to indium oxide (ITO), metal nanowire transparent conductive electrodes (TCEs) have attracted more and more attention. Here, a facile method that can be applied to the synthesis of a variety of metal/bimetallic nanowires has been proposed. Metal/bimetallic nanowires synthesized through this method show high aspect ratios and great dispersibility, which makes them ideal building blocks for transparent electrodes. The synthesis mechanism is discussed in-depth to give a theoretical basis of morphology control of metal nanostructures in organic synthesizing systems. TCEs with high flexibility, excellent optical–electrical performance as well as outstanding anti-thermal and anti-moisture stability are constructed. To the best of our knowledge, this is the first work on synthesizing multiple metal/bimetallic nanowires through one method.

1. Introduction

As the development of electronic industry and energy conversion equipments, high-performance transparent conductive materials are in great demand. The dominant transparent conductive material used today is tin-doped indium oxide (ITO),[1] whose applications in future flexible electronics are limited by its scarcity of supply and brittle nature.[1–4] Among the potential replacements of ITO, metal nanostructures have shown preponderant optical, mechanical, and electrical properties, which make them the most competitive ones, and many methods for fabricating metal nanostructure devices have been reported.[5–7] Metal nanostructures designed for transparent conductors in recent years mainly include metal mesh and metal nanowires, amid which the later ones have gained broad interest since they are easy to synthesize and well suited for constructing large-scale films with low cost techniques, such as roll-to-roll coating. Many methods for synthesizing and fabricating metal nanowire devices have been reported.

Precise control of the morphology of metal nanostructures is the premise for their applications, and many efforts have been devoted to it.[8–12] Based on the established crystal growth theory, several methods have been proposed to synthesize metal nanowires, mainly including electrodeposition,[13] chemical vapor deposition,[14] and chemical reduction in solutions with the presence of capping agent.[2,11,15] Among these methods, nanowires prepared by wet chemical methods have the highest aspect ratio, which is essential to the fabrication of high-performance transparent conductive films. A growing process of 1D nanocrystals needs strict control over the nucleation and crystal growth rate, which will be influenced by several factors, such as reducing agent, reacting temperature, directing agent, the concentration of metal ions etc. However, the fact that different metals have diverse reduction potentials hinders the efforts of finding a reaction system in which the reaction rates of different metals can all be precisely controlled. In order to avoid this problem, researchers use different reaction systems for different metal or multimetallic nanowires. For example, silver nanowires (Ag NWs) are generally synthesized in poly(vinyl pyrrolidone) solutions with ethylene glycol as the reducing agent,[16] while hydrazine

X. Wang, Dr. R. Wang, Dr. L. Shi, Prof. J. Sun
State Key Laboratory of High Performance Ceramics and Superfine Microstructure
Shanghai Institute of Ceramics
Chinese Academy of Sciences
Shanghai 200050, China
E-mail: wangranran@mail.sic.ac.cn
jingsun@mail.sic.ac.cn

DOI: 10.1002/smll.201501314

hydrate is commonly used as reducing agent in synthesizing copper nanowires (Cu NWs).[5]

Unfortunately, metal/bimetallic nanowires synthesized in different reaction systems are usually different in diameter (from 16 to ≈70 nm),[12,17] degree of crystalline, surface morphology, particle contents, and residue organics. These differences not only influence the following steps of electrodes fabrication, but also influence the electrical and optical performances of the electrodes made of these nanowires. As a result, it is difficult for the researchers to systematically evaluate the performances of different metal/bimetallic nanowires in the form of transparent electrodes. Moreover, the nanowires synthesized in aqueous system are usually poorly dispersed, and some of these processes must be operated in inert atmosphere to avoid the oxidation of nanowires.[10] These shortcomings of existing synthesis methods promote the search for new synthesis methods. Here, we reported a facile method, which can be applied to the synthesis of various metal/bimetallic nanowires. In order to obtain 1D metal nanostructure with large aspect ratio, we choose a weak reducing agent and a strong complexing agent to slow down the nucleation and crystal growth rate. Specifically, hexadecylamine (HDA) was chosen as the solvent and reducing agent considering its mild reducibility and preferential adsorption, while cetyl triamoninum bromide (CTAB) worked as the complexing agent. Ag NWs and Cu NWs with similar average diameter (50–60 nm), length (135 μm), dispensability and surface morphology were synthesized through the one reacting system, so did Cu–Ni (with average diameter of 100 nm and length of 140 μm) and Cu–Ag (with average diameter of 80 nm and length of 130 μm) bimetallic nanowires (Cu–Ni NWs and Cu–Ag NWs) (Figure S1, Supporting Information). The mechanisms were profoundly discussed. The optical–electrical properties and stability of transparent conductive electrodes (TCEs) based on these four metal/bimetallic nanowires were systematically evaluated. Moreover, the underlying causes influencing their performance were anatomized, which is of great significance to fabricate highly conductive, transparent, and stable electrodes.

2. Results and Discussion

The synthesis procedure is quite simple. First, HDA and CTAB were mixed and melted, metal source was then added into the solvent, after being kept at the temperature of 130 °C–200 °C for 6 h, precipitations were obtained at the bottom of the reaction vessels. The precipitations were then separated from the reaction system, and dispersed in toluene for further characterization.

Using silver acetylacetonate or copper acetylacetonate as the metal source, we can get Ag NWs or Cu NWs through the method showed above. The nanowires are well dispersed in toluene with an average diameter of 50–60 nm. Most of the aspect ratios of Ag NWs can be as high as 1000, some of the aspect ratios of Cu NWs can reach 2500 or even 3000, both of them show higher aspect ratios as well as thinner diameters compared to the nanowires reported previously.[1,11,15,18–21] The insets of **Figure 1**A,B show that the nanowires have uniform diameters and smooth surface, which is quite essential to the optimization of metal nanowire transparent conductive films. The XRD patterns indicate the pure nature of these two nanowires.

Based on a serious of phenomena we observed from the synthesizing process of Cu NWs and Ag NWs, a synthesis mechanism was proposed (**Scheme 1**). First, the mixing of HDA and CTAB at certain ratios will form a tubular liquid crystal phase as reported before,[12] which will provide channels for the growth of 1D structures. Then, silver or copper acetylacetonate was added into the liquid mixture. $M_x(acac)_y$ was chosen as the metal source since they have a stable coordination structure and can release metal ions slowly. Typically, both oxygen atoms bind to the metal to form a six-membered chelate ring as shown in scheme 1. When added to the melted HDA at high temperature, the chelate ting will be attacked by -NH_2 groups and will be open,[22] resulting in the release of M^{n+} ions. M^{n+} ions will be then coordinated with Br (I) ions dissociated from CTAB, which have been confirmed by the color change from dark green to orange yellow during the synthesizing process of Cu NWs (Figure S2, Supporting Information). The dissociation of CTAB would break the electrostatic equilibrium of the tubular micelle, and $[M_xBr_y]^{n-}$ complex ions with negative charges will be then attracted into the channel to balance the positive charges of CTA^+ ions. After that, the $[M_xBr_y]^{n-}$ complex will be reduced by HDA with or without the assistance of catalyst, forming metal clusters and building particles within the tubular channels. We further analyzed the remaining organic compounds by GC-MS when the synthesizing process was over. In addition to HDA, hexadecanenitrile was also found (Figure S3, Supporting Information). It is believed that, via catalyzing by Pt nanoparticles or Ag/Ni clusters, M^{n+} will gain electrons from HDA, and dehydrogenation of HDA will occur and resulting in the formation of hexadecanenitrile and M(0). Because of the preferential adsorption of HDA and Br^- on some particular planes, confined growth of the building clusters and particles happens and leads to the formation of Cu or Ag nanowires with high aspect ratios.

Despite the wonderful properties of Cu or Ag nanowires, they still have some intrinsic shortcomings such as high cost of silver and poor stability of copper. Metal nanowires consisted of two or more metals can take advantage of both components, like corrosion resistance of nickel, conductivity of copper and electrocatalyst properties of noble metals. This habitude gives bimetallic/multimetallic nanowires the potential of becoming ideal building blocks for high- performance TCEs. Here, we further developed this method to synthesize Cu–Ni NWs and Cu–Ag NWs by adding nickel acetate or silver acetylacetonate into the reaction system.

The SEM image and dark field microscopy image of Cu–Ni NWs (**Figure 2**) show that the nanowires synthesized through this method have high aspect ratios (mostly higher than 1000) (Figure S1, Supporting Information), uniform diameters (≈140 nm) and excellent dispersibility. Compared to the Cu–Ni NWs previously reported,[2] the nanowires we got have a smooth surface and are well crystallized (Figure S4, Supporting Information), and it was the first time to report

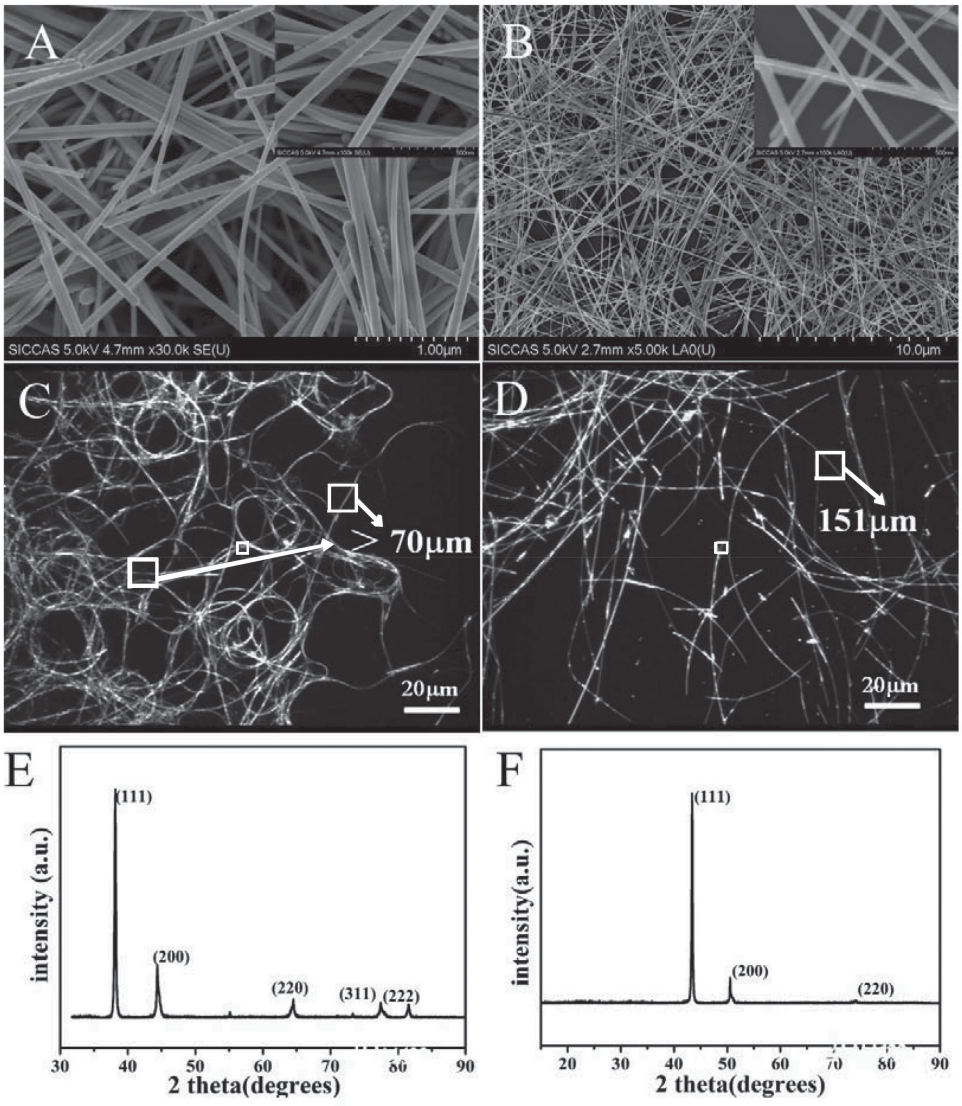

Figure 1. A) SEM image of Ag NWs. The inset of (A) is a high-resolution SEM image of Ag NWs. B) SEM image of Cu NWs. The inset of (B) is a high-resolution SEM image of Cu NWs. C,D) Dark field optical microscopy images of Ag NWs and Cu NWs. E,F) XRD spectra of Ag NWs and Cu NWs.

bimetallic nanowires with such high length and smooth surface simultaneously. This can be contributed to the fact that we used a much more moderate reaction system and achieved better control of the deposition of copper and nickel atoms compared to the hydrazine reduction system reported beforehand.[2] Figure 2 also gives the images of the distribution of two elements in Cu–Ni NWs. It confirms that nickel atoms were uniformly wrapped around the copper core. Interpenetration happened between the copper core and the nickel shell and finally formed uniform bimetallic nanowires with a copper-rich core and a nickel-rich shell (Figure 2C–F). By changing the amount of nickel acetate and reacting time, the percentage of nickel element in a Cu–Ni NW could be well controlled in a range from 5% to 60%, this can be easily explained by the fact that copper and nickel are completely miscible in all proportions.

The formation mechanisms of Cu–Ni NWs was different from metal nanowires showed above, it was mainly consist of three types according to previous reports: heterogeneous growth, galvanic replacement, and co-reduction, and different formation mechanisms lead to different bimetallic structures.[23] Particularly, in some reaction systems, more than one growth theories need to be used to explain the formation mechanism. In our reaction system, two stages were involved during the synthesis of Cu–Ni NWs. The first stage refers to the pre-formation of copper core, the process of which is similar to that of synthesizing Cu NWs. The first stage lasts for several hours, following by elevating temperature and the addition of nickel acetate, which opens up a new reaction stage. In the second stage, preformed copper cores can serve as reactive precursors to catalyze the reduction of remaining copper ions and nickel ions[24] and work as a template for heterogeneous growth of bimetallic nanowires. At a proper temperature, copper ions and nickel ions are co-deducted, and then co-deposited onto the copper cores, forming a nickel-rich shell and copper-rich core structure. As

www.MaterialsViews.com

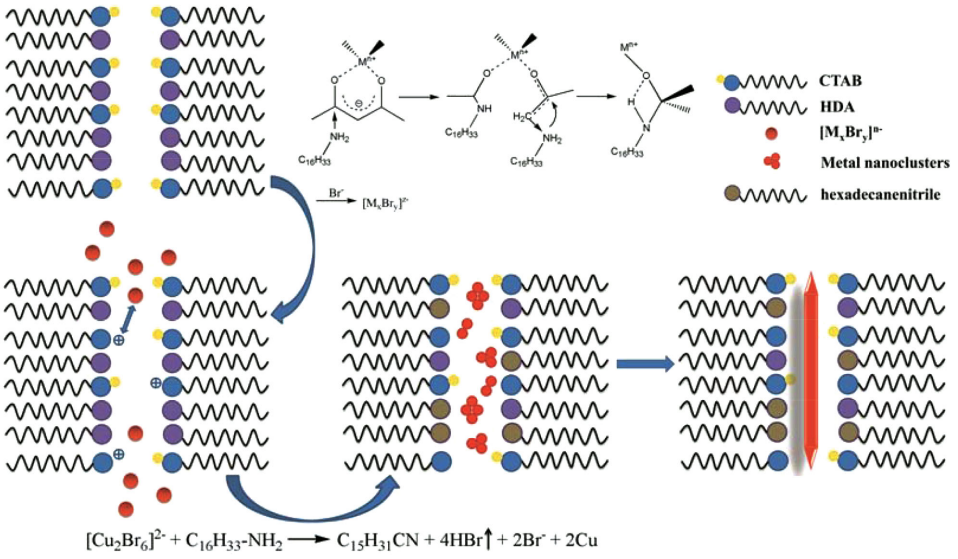

Scheme 1. Schematic diagram of the synthetic procedure for metal nanowires.

copper and nickel have similar lattice constants and the fact that they are miscible in any proportion, the elemental composition of the nanowires can be tuned in a wide range.

According to the formation mechanism of copper–nickel nanowire, we presume the formation of copper–nickel solid solution alloy at the nickel-rich shell of a nanowire. To confirm this conjecture, we tested the XRD spectrum of copper-nickel nanowires with different nickel atom contents of 14%, 29%, and 55% (Figure S4, Supporting Information). Apart from the main peaks indexed as the face-centered cubic structure of Cu, a broad peak can also be observed between the standard peaks of Cu (JCPDS no. 04-0836) and Ni (JCPDS no. 04-0850). As the nickel atom contents increase, this peak moves to a high angle, indicating the formation of copper–nickel solid solution alloy.

We can also synthesize Cu–Ag NWs with uniform diameters (≈80 nm) and high aspect ratios through this method (**Figure 3** and Figure S1, Supporting Information). Differently, the temperature should be lowered after the pre-formation of copper core, considering the higher redox potential of silver. Unlike the smooth surface of Cu–Ni NWs, the surfaces of Cu–Ag NWs are quite rough with a lot of small particles along the nanowires. This may be caused by a different formation mechanism. The redox potential of silver is higher than copper. Similarly to the copper-noble metal bimetallic nanostructures reported previously,[25–27] galvanic replacement rather than co-reduction mechanism is used to explain the formation of copper–silver nanowires. In the reaction system, preformed copper nanowires work as the template. Upon the addition of Ag(acac), copper atoms located at the outer surface of the nanowires are partly oxidized and replaced by silver atoms. This replacement process preferentially happened at the defect sites and is too fast for crystal growing process, which leads to the coarse surface of the Cu–Ag NWs. Instead of forming solid solution alloy like Cu–Ni NWs, copper and silver exists in a single metal form. Standard peaks of Cu (JCPDS no. 04-0836) and Ag (JCPDS no. 04-0783) can be seen in the XRD spectrum of Cu–Ag NWs (Figure S5, Supporting Information).

Unlike the synthesis methods showed ahead, we propose a versatile method

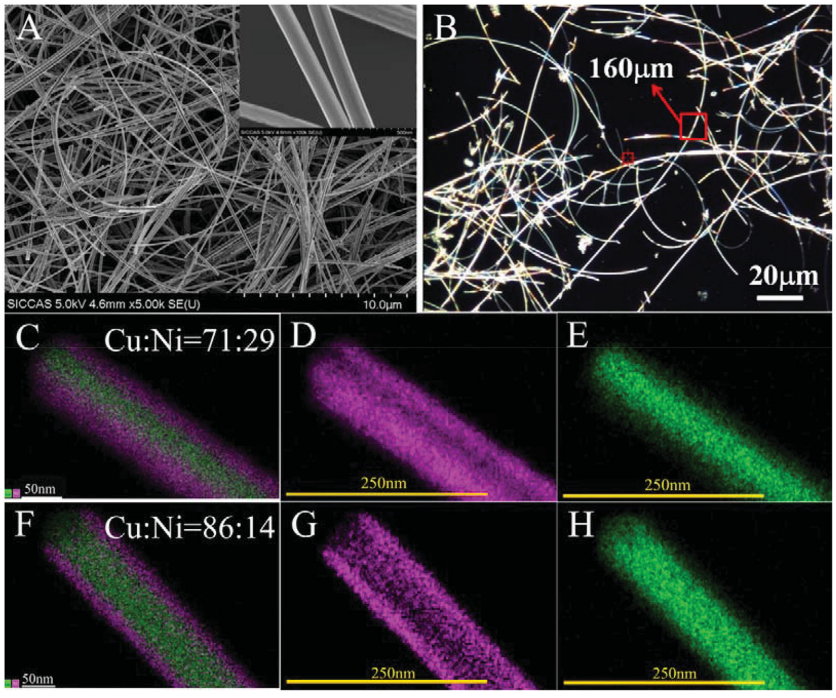

Figure 2. A) SEM image of Cu-Ni NWs. The inset of A is a high-resolution SEM image of Cu-Ni NWs. B) Dark-field optical microscopy images of Cu–Ni NWs. C–H) Energy-dispersive X-ray spectroscopy images of Cu–Ni NWs with different contents of nickel.

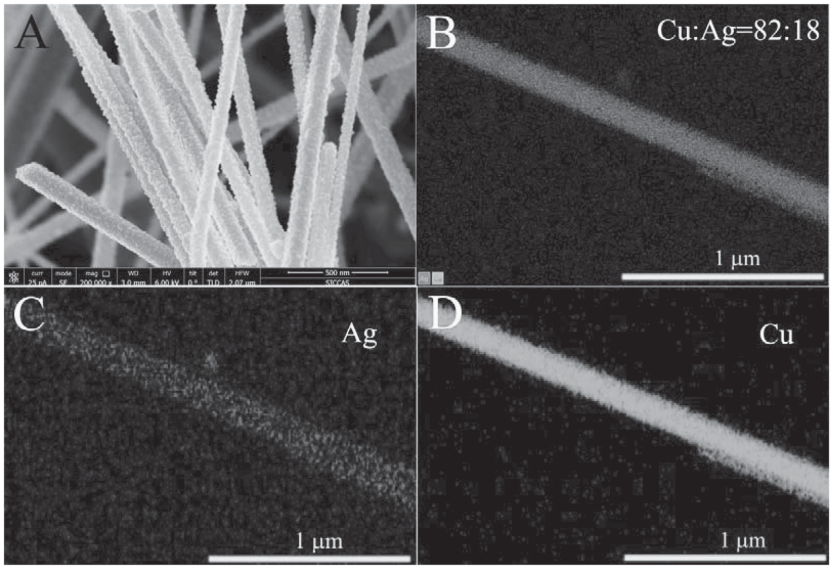

Figure 3. A) SEM image of Cu–Ag NWs. B,C,D) Energy-dispersive X-ray spectroscopy images of Cu–Ag NWs with silver atom content of 18%.

which is well suited for synthesizing various metal/bimetallic nanowires. Most of the nanowires are monodispersed in common organic solvents, such as toluene and isopropanol. Besides, the nanowires exhibit superior stability than those synthesized in aqueous solutions, and can be preserved under ambient atmosphere without the protection of reducing agent. Cu and Ag NWs show similar diameters, length, and surface morphology, so do Cu–Ni and Cu–Ag bimetallic NWs, which facilitate the evaluation of their intrinsic properties as transparent electrodes without the inferences of other factors.

In order to evaluate their optical–electrical properties, these metal/bimetallic nanowires were prepared into films by vacuum filtration, followed by post annealing or plasma treatment to remove the residue organics and to facilitate nanowire junctions welding together. Interestingly, the silver nanowires we got through this method show great conductivity in the form of a film without any further treatment, which makes it easier for large-scale film production than the silver nanowires reported previously.[28]

Figure 4A shows the specular transmittance spectra and camera photographs of the transparent films studied. All of these TCEs show gentle slops in the visible range, while for Ag and Cu–Ag NW TCEs, the descents of transmittance from 800 to 400 nm is numerically stronger, which may be caused by the surface plasmon resonance absorption of silver. A valley can be seen in the vicinity of 400 nm for the spectrum of Ag NW and Cu–Ag NW TCEs, close to the LSPR wavelength (scattering peak position) of silver nanostructures. The valley for Cu–Ag NW TCE shows a broader shape and a red-shift center compared to Ag NW TCE, which optically indicates the formation of silver nanoparticles around the copper nanowires. The red color of Cu NW films (Figure 4A) seriously limited their applications in displays, but the formation of Cu–Ni and Cu–Ag NWs provides an effective solution to the problem. The neutral colors of bimetallic nanowire TCEs and Ag NW TCEs make them better candidates in flat panel displays. Figure 4B gives the transmittance-sheet resistance curves of these four metal/bimetallic nanowire TCEs. Among these nanowires, Ag NW TCEs show the highest conductivity (Figure 4B) (20 Ω sq^{-1}–90.7% T), which is comparable to the best ITO. This is reasonable considering the highest electrical conductivity of silver. Cu and Cu–Ag NW films show similar performances, typically a sheet resistance of 20 Ω sq^{-1}–85% T (15 Ω sq^{-1}–85% T for the best), which outperform previous reports. Cu--Ag NW films do not exhibit superior performance than Cu NW films as expected, which can be attributed to the nonuniform silver shell and the increased diameter. The optical–electrical performance of Cu–Ni NW TCEs is inferior to the other three nanowire films due to the low conductivity of nickel. However, the sheet resistance of 30–40 Ω sq^{-1}–85% T can also meet the criteria of transparent electrodes in touch screen (≤500 Ω sq^{-1}–85% T) and is far below that of single-walled CNT networks.

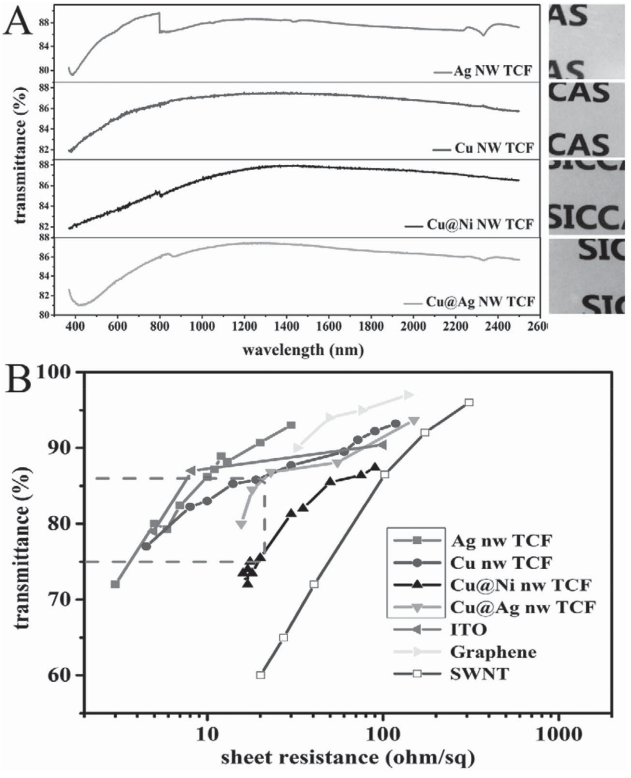

Figure 4. A) Plots of specular transmittance versus wavelength and camera photographs for films with similar transmittance (T% ≈ 85 %, λ = 550 nm) and of ultralong Ag NWs, Cu NWs, Cu–Ni NWs (Cu:Ni = 62:38) and Cu–Ag NWs (Cu:Ag = 82:18). B) Plots of sheet resistance for films of Ag NWs, Cu NWs, Cu–Ni NWs (Cu:Ni = 62:38), Cu–Ag NWs (Cu:Ag = 82:18), ITO,[31,32] SWNT[31,33] and graphene[31] versus transmittance (λ = 550 nm). The area surrounded by the dash line indicates the T-Rs target region for transparent conductive electrode applications.

The figure of merit (FOM)-specific value of DC conductivity (σ_{dc}) and optical conductivity (σ_{op}) is often used to evaluate the conductive performance of metal nanowire conductive films as applicable electrodes. A higher FOM represents a lower sheet resistance at higher transmittance, which is preferred in transparent conductive films.

$$T = \left(1 + \frac{188.5}{R_S}\frac{\sigma_{op}}{\sigma_{dc}}\right)^{-2} \quad (1)$$

According to Equation (1),[1,28] the FOM of our samples were 158 (Cu NW TCEs), 46 (Cu–Ni NW TCEs), 250 (Ag NW TCEs), and 125 (Cu–Ag NW TCEs), exceeding previously reported results, such as 125 for Cu NW, 26.5 for single-walled CNTs.[29] The high FOM can be attributed to the high aspect ratio and the well-crystallized structure of the nanowires.

Apart from conductivity, stability is also an important factor in the evaluation of metal nanowire TCEs. Here, we use the normalized change in the sheet resistance R/R_0 of metal/bimetallic nanowire films versus time as an estimate of stability. The time it takes for R/R_0 to double is used as a test standard. Films with similar transmittance (85% T) are used as test objects to avoid the influence of thickness. According to **Figure 5**A, all these metal/bimetallic nanowire TCEs remain stable at room temperature in a month, much better than previous reports, which again proved the superiority of this synthesis method. However, the oxidation will be speed up at elevated temperatures. As seen from Figure 5B, Cu NW TCEs oxidized rapidly and lost their conductivity, while R/R_0 of Cu–Ag NW and Ag NW TCEs doubled in 5 d and 15 d, respectively. By comparison, Cu–Ni NW TCEs showed remarkable stability in a month at 65 °C. The uniform and stable nickel shell is mainly responsible for such excellent performance. Considering the heat generation of electronic products, stability TCEs at elevated temperature is of great importance.

In addition to temperature, humidity is another important factor to influence the oxidation process of metal nanowires. When the relative humidity was elevated to 85% at room temperature, TCEs based on Cu NWs oxidized rapidly. This is mainly ascribed to the reaction of copper with CO_2 and H_2O. Covering with nickel and silver layer can hinder the corrosion of Cu NWs from moisture effectively, as shown in Figure 5C. This is the first time to give a comprehensively evaluation of the performances of Cu–Ag NWs in the form of transparent electrodes. Although their optical–electrical performances were similar to that of Cu NW electrodes, they exhibited much better anti-thermal and anti-moisture stability than Cu NWs TCEs. Unfortunately, the cover layer protection could not show much success anymore in the environment of both high humidity and high temperature (Figure 5D,E). By contrast, Ag NW TCEs exhibited superior stability in humid environment, since they were not apt to react with moisture. The stability of metal nanostructures might be the biggest obstacle in their usage. The excellent anti-thermal oxidation ability of nickel layer and the anti-moisture corrosion function of silver layer showed great enlightenment on seeking ways to enhance the weather ability of metal nanowire TCEs. It is believed that forming bimetallic or even multi-metallic nanowires might be a promising way to enhance the conductivity and weather stability, as well as lower the cost of metal nanowires TCEs.

We further tested the stability of nanowire films under cyclical comprehensive and tensile bending (**Figure 6**). Flexible electrodes based on poly(acrylate) substrates were fabricated through a method reported previously,[30] The sheet resistance of all these nanowire composite films exhibited almost no increase after 1000 bends, which indicates the

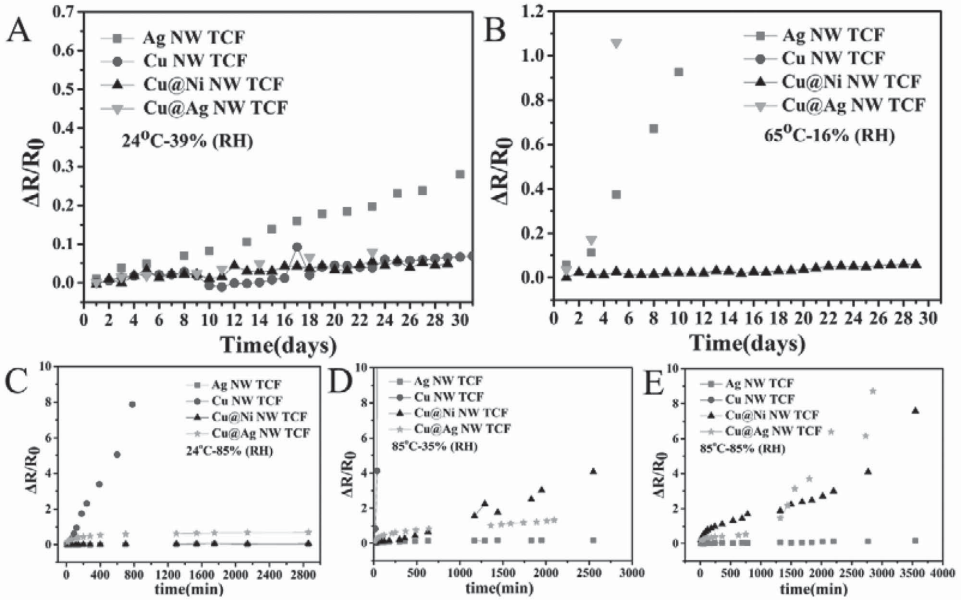

Figure 5. Plots of sheet resistance versus time for transparent conductive films of Cu NWs, Ag NWs, Cu–Ni NWs (Cu:Ni = 62:38) and Cu–Ag NWs (Cu:Ag = 82:18) (T% ≈ 85%, λ = 550 nm) stored at the temperature of A) 24 °C and B) 65 °C; Plots of sheet resistance versus time for films of Cu NWs, Ag NWs, Cu–Ni NWs (Cu:Ni = 62:38) and Cu–Ag NWs under different temperatures and humidity conditions: C) 24 °C–85% (RH); D) 85 °C–35% (RH); E) 85 °C–85% (RH).

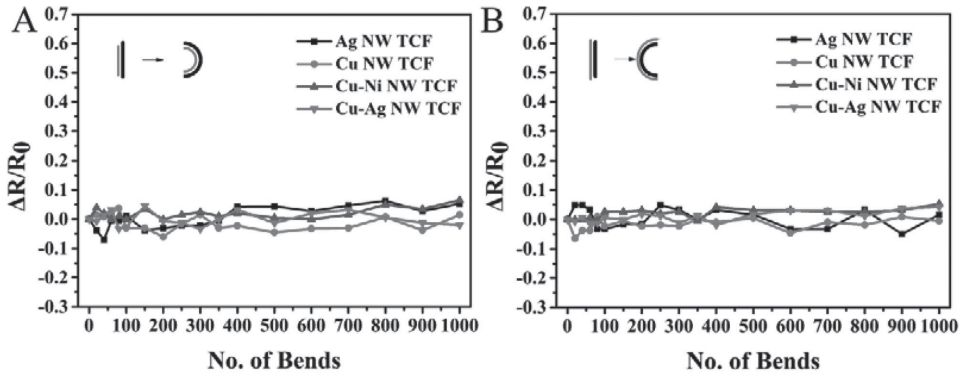

Figure 6. Plots of sheet resistances versus number of bends for Ag NW TCEs (6.13 Ω sq^{-1}), Cu NW TCEs (13.6 Ω sq^{-1}), Cu–Ni NW TCEs (21.3 Ω sq^{-1}) (Cu–Ni NWs with Ni atom content of 38%) and Cu–Ag NW TCEs (15.6 Ω sq^{-1}) (Cu–Ag NWs with Ag atom content of 18%) with similar transmittance (T% ≈ 80%, λ = 550 nm).

excellent flexibility of the nanowire TCEs. The highly flexible metal/bimetallic nanowires with high aspect ratios and their combination with elastic substrates endow the nanowire TCEs with outstanding flexibility and make sure that they can be used in flexible electronic devices.

3. Conclusion

In summary, we have introduced a versatile method that can be used to synthesize a variety of metal/bimetallic nanowires. An in-depth discussion of the reaction mechanism was also proposed, which provide theoretical basis for the morphology control of metal/bimetallic nanostructures. The metal/bimetallic nanowires synthesized by this method have high aspect ratio, smooth surface, and outstanding dispersibility. TCEs made by these metal or bimetallic nanowires were evaluated systematically, which demonstrated the most superior conductivity and anti-moisture stability of Ag NWs, as well as excellent anti-thermal stability of Cu-Ni NWs in the long run. These discoveries are great inspirations to develop novel building blocks for high-performance and low-cost TCEs. Moreover, this synthesis system can be expanded to more metal, bimetallic or even multi-metallic nanowire fabrications.

4. Experimental Section

Pre-reaction: HDA (8 g) and CTAB (0.5 g) were mixed and melted at the temperature of 180 °C to form a clear and colorless solution.

Preparation of Ag NWs: The pre-prepared solution was cooled to 140 °C in an oil bath. Silver acetylacetonate (50 mg) was dispersed in ethanol and added to the reaction system. The solution was then kept at 140 °C for 10 h until a large amount of light gray precipitation appeared. Ag NWs were separated and washed by toluene through centrifugation and kept in toluene for further characterization.

Preparation of Cu NWs: Cu NWs were synthesized in a similar way. Copper acetylacetonate was added into the pre-prepared solution, and after being kept at 180 °C for 30 min, catalysts were added to the reaction system to promote the reduction of copper ions. With the help of catalysts, copper nanowires began to form in the system at the temperature of 180 °C. The solution was then kept at 180 °C for 12 h and cooled to room temperature. Red precipitation of Cu NWs can be seen at the bottom of the reaction vessel. After being washed and dispersed by toluene, the Cu NWs were stored at room temperature. Typically, platinum nanoparticles with the size of 5 nm were added as the catalyst. In addition to platinum nanoparticles, silver or nickel clusters also can catalyze the reduction of Cu (II) ions.

Preparation of Cu–Ni NWs: Cu–Ni NWs were synthesized by a modified synthesis process of copper nanowires. After the synthesis process of copper nanowires was aged for 10 h, nickel acetate (0.2–1.3 g) was added to the solution and the temperature suddenly increased to 210 °C. The solution was then kept at this temperature for another 2 h. The separating and washing process was similar to Cu NWs and Ag NWs.

Preparation of Cu–Ag NWs: The synthesis process of Cu–Ag NWs was similar to Cu–Ni NWs. Differentially, we used silver acetylacetonate (30–50 mg) as the silver source, and the temperature for the reaction was 90 °C.

Preparation of Metal/Bimetallic Nanowire Transparent Films: Metal/bimetallic nanowires were dispersed in toluene to form a homogenous suspension. After films formed through vacuum filtration, it was transferred to a substrate (glass slid, silicon wafers, PET, etc) through a hot-pressing transfer process. During this process, nitrocellulose membrane (Millipore membrane, 0.22 μm GSWP) is used as the filtration membrane. A deposited film was placed on the substrate and kept at 80 °C for an hour in a vacuum oven with a 3 kg weight on the top, then the membrane was removed through acetone liquid bath.

Characterization: The transmittance and sheet resistance of metal/bimetallic nanowire TCFs were tested through a UV/VIS spectrometer (Lambda 950, PerkinElmer) and a four-point probe (Loresta-EP MCP-T 360). The aging test was carried out in a constant temperature and humidity test chamber (Espec Corp SH-222). During the aging test, we used different temperatures and humidity conditions of 24 °C–85% (RH), 85 °C–35% (RH) and 85 °C–85% (RH).

GC-MS analysis was carried out on an Agilent 7890A instrument.

In order to show the average length of the nanowires, the nanowires were imaged through a dark-field optical microscope.

The micromorphology of these nanowires and EDS analysis was conducted with a field-emission scanning electron microscopy (Magellan 400) and a transmission electron microscopy (JEM-2100F). The crystallographic analysis was carried out on an X-ray diffractometer (Rigaku D/max 2550 V).

Flexible electrodes were fabricated by on a cured poly(acrylate) substrate through the method reported previously.[30]

Conflict of Interest

The authors declare no competing financial interest.

Supporting Information

Supporting Information is available from the Wiley Online Library or from the author.

Acknowledgement

This work was supported by Technology Innovation Project of Shanghai Institute of Ceramics (Grant Nos.Y41ZC6160G and Y31ZC6160G), National Natural Science Foundation of China (Grant No. 61301036), and Shanghai Municipal Natural Science Foundation (Grant No. 13ZR1463600).

[1] D. S. Hecht, L. Hu, G. Irvin, *Adv. Mater.* **2011**, *23*, 1482.
[2] A. R. Rathmell, M. Nguyen, M. Chi, B. J. Wiley, *Nano Lett* **2012**, *12*, 3193.
[3] Y. H. Kim, C. Sachse, M. L. Machala, C. May, L. Müller-Meskamp, K. Leo, *Adv. Funct. Mater.* **2011**, *21*, 1076.
[4] K. Ellmer, *Nat. Photonics* **2012**, *6*, 809.
[5] A. R. Rathmell, B. J. Wiley, *Adv. Mater.* **2011**, *23*, 4798.
[6] J. W. Liu, J. L. Wang, Z. H. Wang, W. R. Huang, S. H. Yu, *Angew. Chem. Int. Ed. Engl.* **2014**, *53*, 13477.
[7] H.-Y. Shi, B. Hu, X.-C. Yu, R.-L. Zhao, X.-F. Ren, S.-L. Liu, J.-W. Liu, M. Feng, A.-W. Xu, S.-H. Yu, *Adv. Funct. Mater.* **2010**, *20*, 958.
[8] X. Xia, Y. Wang, A. Ruditskiy, Y. Xia, *Adv. Mater.* **2013**, *25*, 6313.
[9] M. Jin, G. He, H. Zhang, J. Zeng, Z. Xie, Y. Xia, *Angew. Chem. Int. Ed. Engl.* **2011**, *50*, 10560.
[10] H. Guo, Y. Chen, H. Ping, J. Jin, D. L. Peng, *Nanoscale* **2013**, *5*, 2394.
[11] K. E. Korte, S. E. Skrabalak, Y. Xia, *J. Mater. Chem.* **2008**, *18*, 437.
[12] D. Zhang, R. Wang, M. Wen, D. Weng, X. Cui, J. Sun, H. Li, Y. Lu, *J. Am. Chem. Soc.* **2012**, *134*, 14283.
[13] N. J. Gerein, J. A. Haber, *J. Phys. Chem. B* **2005**, *109*, 17372.
[14] C. Kim, W. Gu, M. Briceno, I. M. Robertson, H. Choi, K. Kim, *Adv. Mater.* **2008**, *20*, 1859.
[15] M. Mohl, P. Pusztai, A. Kukovecz, Z. Konya, J. Kukkola, K. Kordas, R. Vajtai, P. M. Ajayan, *Langmuir* **2010**, *26*, 16496.
[16] S. Coskun, B. Aksoy, H. E. Unalan, *Cryst. Growth Des.* **2011**, *11*, 4963.
[17] H. Guo, N. Lin, Y. Chen, Z. Wang, Q. Xie, T. Zheng, N. Gao, S. Li, J. Kang, D. Cai, D. L. Peng, *Sci. Rep.* **2013**, *3*, 2323.
[18] J. Lee, P. Lee, H. Lee, D. Lee, S. S. Lee, S. H. Ko, *Nanoscale* **2012**, *4*, 6408.
[19] C. Yang, H. Gu, W. Lin, M. M. Yuen, C. P. Wong, M. Xiong, B. Gao, *Adv. Mater.* **2011**, *23*, 3052.
[20] Z. Yu, Q. Zhang, L. Li, Q. Chen, X. Niu, J. Liu, Q. Pei, *Adv. Mater.* **2011**, *23*, 664.
[21] J. H. Lee, P. Lee, D. Lee, S. S. Lee, S. H. Ko, *Cryst. Growth Des.* **2012**, *12*, 5598.
[22] N. Pinna, G. Garnweitner, M. Antonietti, M. Niederberger, *J. Am. Chem. Soc.* **2005**, *127*, 5608.
[23] W. Li, L. Kuai, Q. Qin, B. Geng, *J. Mater. Chem. A* **2013**, *1*, 7111.
[24] R. E. Cable, R. E. Schaak, *Chem. Mater.* **2007**, *19*, 4098.
[25] L. Wang, H. Chen, M. Chen, *Mater. Res. Bull.* **2014**, *53*, 185.
[26] M. Mohl, D. Dobo, A. Kukovecz, Z. Konya, K. Kordas, J. Wei, R. Vajtai, P. M. Ajayan, *J. Phys. Chem C* **2011**, *115*, 9403.
[27] Z. Jiang, Q. Zhang, C. Zong, B.-J. Liu, B. Ren, Z. Xie, L. Zheng, *J. Mater. Chem.* **2012**, *22*, 18192.
[28] S. Zhu, Y. Gao, B. Hu, J. Li, J. Su, Z. Fan, J. Zhou, *Nanotechnology* **2013**, *24*, 335202.
[29] F. Mirri, A. W. K. Ma, T. T. Hsu, N. Behabtu, S. L. Eichmann, C. C. Young, D. E. Tsentalovich, M. Pasquali, *ACS Nano* **2012**, *6*, 9737.
[30] Y. Cheng, S. Wang, R. Wang, J. Sun, L. Gao, *J. Mater. Chem. C* **2014**, *2*, 5309.
[31] F. Bonaccorso, Z. Sun, T. Hasan, A. C. Ferrari, *Nat. Photonics* **2010**, *4*, 611.
[32] T. M. Barnes, M. O. Reese, J. D. Bergeson, B. A. Larsen, J. L. Blackburn, M. C. Beard, J. Bult, J. van de Lagemaat, *Adv. Energy Mater.* **2012**, *2*, 353.
[33] H.-Z. Geng, K. K. Kim, K. P. So, Y. S. Lee, Y. Chang, Y. H. Lee, *J. Am. Chem. Soc.* **2007**, *129*, 7758.

Received: May 8, 2015
Published online: July 14, 2015